Ecohydrological Optimality in Northeast China Transect

Zhentao Cong[1,2], Qinshu Li[1,2], Kangle Mo[1,2], Lexin Zhang[1,2], Hong Shen[1,2]

[1]Department of Hydraulic Engineering, Tsinghua University, Beijing, 100084, China
[2]State Key Laboratory of Hydroscience and Engineering, Beijing, 100084, China

5   *Correspondence to*: Zhentao Cong (congzht@tsinghua.edu.cn)

Abstract. Northeast China Transect (NECT) is one of the International Geosphere-Biosphere Program (IGBP) terrestrial transects, where there is a significant precipitation gradient from east to west, as well as a vegetation transition of forest-grasslands-dessert. It is remarkable to understand vegetation distribution and dynamics under climate change in this transect. We take canopy cover (M), derived from Normalized Difference Vegetation Index (NDVI), as an index to describe the

10   properties of vegetation distribution and dynamics in NECT. In Eagleson's ecohydrological optimality theory, the optimal canopy cover (M^*) is determined by the trade-off between water supply depending on water balance and water demand depending on canopy transpiration. We apply Eagleson's ecohydrological optimality method in NECT based on data from 2000 to 2013 to get M^*, which is compared with M from NDVI to further discuss the sensitivity of M^* to vegetation properties and climate factors. The result indicates that the average M^* fits the actual M well (for forest, $M^* = 0.822$ while $M = 0.826$;

15   for grassland, $M^* = 0.353$ while $M = 0.352$; the correlation coefficient between M and M^* is 0.81). Results of water balance also match the field-measured data in references. The sensitivity analyses show that M^* decreases with the increase of LAI, stem fraction, and temperature, while increases with the increase of leaf angle and precipitation amount. The Eagleson's ecohydrological optimality method offers a quantitative way to understand the impacts of climate change on canopy cover, and provides guidelines for eco-restoration projects.

20   **Key Words:** NECT; canopy cover; optimality; ecohydrology, climate change

1 Introduction

Transect studies play an important role in understanding the role of the terrestrial biosphere in global change (Koch et al, 1995a). The Global Change and Terrestrial Ecosystems (GCTE) project of International Geosphere-Biosphere Program (IGBP) has chosen fifteen transects along with environmental or land-use gradients, aiming at understanding how these factors

25   influence terrestrial ecosystem and the interaction between biosphere and atmosphere (Koch et al, 1995; Canadell et al, 2002; Austin and Sala, 2002). Northeast China Transect (NECT) was identified as one of the IGBP transects in 1993, with precipitation/moisture as the main driving climate factor (Ni and Zhang, 2000; Zhang and Zhou, 2011). Along with the moisture gradient, vegetation types vary gradually from forests in the east, to the cropland in the middle, and grassland and bare soil in the west.

Vegetation plays an important role in terrestrial ecosystems. It strongly influences the exchange of energy, substances and moisture between land and atmosphere through photosynthesis, respiration and transpiration (Graetz, 1991; Mcpherson, 2007). At the same time, the vegetation growth condition is largely affected by climate factors, such as precipitation, air temperature and greenhouse gases (Füssler and Gassmann, 2000; Lotsch et al, 2003; Liu and Notaro, 2005).

5   The most common indexes to describe vegetation performance include Normalized Difference Vegetation Index (NDVI) and vegetation canopy cover. NDVI is a linear combination of remotely sensed near-infrared reflectance and red reflectance. It is an index reflecting the greenness of vegetation canopy and photosynthetic activity (Dorman et al, 2013; Fontana et al, 2008; Hmimina et al, 2013). Vegetation canopy cover is defined as the fraction of total ground surface covered by vegetation. Semi-empirical relationships between NDVI and canopy cover were used to derive the possible arithmetic expression of canopy

10   cover (Baret et al, 1995; Carlson and Ripley, 1997; Gutman and Ignatov, 1998; Jiang et al, 2006). With the rising attention of the climate change issue, studies on the relationship between canopy cover and climate factors have been conducted in different regions of the world (Zhou et al, 2001; Schultz and Halpert, 1993; Piao et al, 2011; Park and Sohn, 2010; Li et al, 2002; Wang et al, 2003). Nie et al (2011) used correlation analysis to check the relationship between NDVI and climate factors in NECT, with regression equations given for different time scales. NDVI driven by climate changes varied differently between

15   vegetation types and seasons (Piao et al. 2006). Duan et al. (2011) illustrated that precipitation was the most importance factor in affecting the temporal NDVI patterns over semi-arid and arid regions of China. Peng et al. (2012) found > 70% of the temporal variations in NDVI were contributed by precipitation during the growing season in typical and desert steppes in Northeast China. Mao et al.(2012), however, discovered that the correlation between NDVI and temperature was higher than with precipitation over most parts of Northeast China for all vegetation covers; NDVI presented a downward trend with

20   increased temperature and remarkably decreased precipitation. Further, Yuan et al. (2015) suggested diverse responses of grasslands to precipitation intensities.

Although the statistical models have been established to describe the response of vegetation to climate factors, they cannot express the underlying mechanism of the response quantitatively. Vegetation models were developed to detect how vegetation reacts to climate change based on the biophysical and physiological processes, including plant life cycle, carbon and nitrogen

25   cycles, but many data and parameters were required (Myoung et al, 2011). It is a big challenge to build a simplified model that can describe the mechanism of vegetation response to climate change with relatively few parameters. Fortunately, Eagleson (2002) presents us a theory and method, ecohydrological optimality (Eagleson, 1978a, b, c, d, e, f, g, 1982; Eagleson and Tellers, 1982). In Eagleson's ecohydrological optimality theory, vegetation characteristics, such as leaf angle, leaf area index and canopy cover, are determined by the light, energy, water and soil conditions in long term average state. Different from the

30   models above, Eagleson's ecohydrological optimality theory can not only explore the mechanism of canopy cover distribution, mainly from water balance perspective, but also easy to conduct. The optimality theory provides a new way to explore the quantitative relation between vegetation and climate factors. Despite the fact that Eagleson's work is regarded as the basis for ecohydrology and of great importance (Hotton et al, 1997; Kerkhoff et al, 2004), limited studies have been conducted using

the theory in the practical (Shao et al, 2011; Mo et al, 2015), which is partly due to the limitation of long termtemporal scale, partly due to the difficulty to measure vegetation characteristics.

In Eagleson's ecohydrological optimality theory, the optimal canopy cover ($M*$) is determined by the trade-off between water supply depending on water balance and water demand depending on canopy transpiration. The NDVI data offer us a method to estimate actual canopy cover. If we can verified Eagleson's ecohydrological optimality theory by comparing the optimal canopy cover and remote sensing canopy cover, we can discuss the impact of climate factors and vegetation properties on vegetation cover. From this framework, we can certainly provide some insights in terms of the understanding of climate change impacts on canopy cover dynamics and therefore, can provide useful guidelines for eco-restoration projects, especially for the selection of vegetation species and plant density. Mo et al. (2015) applied this method in Korqin Sand just for one kind of vegetation. In this study, we apply Eagleson's ecohydrological optimality method in NECT based on data from 2000 to 2013 to get $M*$ then compare with M by NDVI, furthermore to discuss the sensitivity of $M*$ to vegetation properties and climate factors.

2 Study area and data

2.1 Study area

The Northeast China Transect (NECT) is one of the mid-latitude IGBP terrestrial transects. It ranges from 42° to 46°N and from 106° to 134°E. The major change gradient is precipitation, which decreases gradually from the eastern mountainous region to the middle farmland and western steppes (Fig. 1). In the east, the annual precipitation is over 600mm/year; meanwhile, in the west, the annual precipitation is under 200mm/year. The land cover types show a significant zonal distribution from east to west: temperate evergreen conifer-deciduous broad leaf mixed forests, deciduous broad leaf forests and woodlands in the east, shrublands and crop in the middle, grassland and bare soil in the west (Fig. 1). In this study, we just focus on the growing season, from May to September.

2.2 Remote sensing data

Monthly NDVI (MOD13A3), yearly Land Cover Types (MCD12Q1) and 8-day LAI (MCD15A2) datasets derived from Moderate-resolution Imaging Spectroradiometer (MODIS) aboard the Aqua and Terra satellite are applied. These satellite data are available on the NASA website (http://reverb.echo.nasa.gov/).

The spatial resolution of NDVI, Land Cover Types and LAI dataset are 1km, 500m and 1km, respectively. Considering the wide longitudinal and latitudinal extends of NECT, these remote-sensed data are resampled to be 10km x 10km. The MODIS Reprojection Tool (MRT) is applied to define coordinate systems for the images. MRT was also used to generate NDVI and LAI data for growing season of each year.

Canopy cover is defined as the fraction of total ground surface covered by vegetation (Eagleson, 2002). Usually a linear transformation of remote-sensed NDVI is used to calculate actual canopy cover (*M*) (Gutman and Ignatov, 1998; Jiang et al, 2006):

$$M = \frac{NDVI - NDVI_{min}}{NDVI_{max} - NDVI_{min}}$$ (1)

5   in which $NDVI_{min}$ is the NDVI of barren soil, and $NDVI_{max}$ is the NDVI of forests. Since the land cove of a fixed grid maybe changed in different year, it was hard to define the real barren soil or the forest areas. We considered the area sensed as barren soil for every year is the barren soil area, and the $NDVI_{min}$ is the spatial average of barren area NDVI. Similarly, the area sensed as forests every year is considered as forests area, and the spatial average of forests NDVI is $NDVI_{max}$. In this study, $NDVI_{min}$ and $NDVI_{max}$ are 0.05 and 0.63 respectively, which means the canopy cover can be regarded as 1 if the NDVI is

10   above 0.63 and as 0 if the NDVI is below 0.05.

2.3 Meteorological data

The meteorological data used in this study from 2000 to 2013 is provided by China Meteorological Data Sharing Service System (http://cdc.cma.gov.cn). The spatial distribution of the 45 meteorological stations is shown in Fig. 1. Atmospheric pressure (P_a), wind speed (W_{nd}), average air temperature (T_a), net radiation (R_n) (estimated by sunshine hours (S_h) and air

15   temperature (Allen, 1998)), relative humidity (R_h), minimum air temperature (T_n), and maximum air temperature (T_m) are required to calculate the potential evapotranspiration by Penman Monteith Equation (Ni and Zhang, 2000; Eagleson, 2002). Kriging interpolation method is applied to generate the spatial distribution of the meteorological factors and potential evapotranspiration. The spatial resolution is 10 km to be consistent with that of remote sensing data.

3 Methodology

20   Eagleson proposed three hypotheses in his ecohydrological optimality theory. He considered that climate and vegetation can influence and adapt to each other on different time scales. First, when climate and soil changes in short time period, the canopy cover will adjust its value to maximize the soil moisture. Second, as the time scales get longer, the species whose potential transpiration efficiency make the soil moisture highest will be selected through natural selection. Third, the soil properties will be altered to ensure the species get their maximum canopy cover (Eagleson, 2002; Hatton et al, 1997). These hypotheses

25   mentioned two important canopy state variables, i.e., the canopy cover (*M*) and canopy conductance (k_v). Canopy conductance is defined as the ratio of potential rates of transpiration E_v and soil surface evaporation E_{ps} (Eagleson, 1978d; Eagleson, 2002):

$$k_v = \frac{E_v}{E_{ps}}$$ (2)

The potential evapotranspiration E_{ps} is calculated by Penman Equation:

$$\lambda E_{ps} = \frac{\Delta R_n + \rho c_p [e_s(T) - e]/r_a}{\Delta + \gamma_0}$$ (3)

30   The canopy transpiration rate E_v is calculated by Penman Monteith Equation:

$$\lambda E_v = \frac{\Delta R_n + \rho c_p [e_s(T) - e]/r_a}{\Delta + \gamma_0 (1 + r_c/r_a)} \tag{4}$$

where

E_{ps} potential rate of evaporation from a wet, simple surface, mm/day

E_v rate of canopy transpiration, mm/day

λ latent heat of vaporization of water = 2500 J/g (at 0 ∘C)

Δ the slope of the saturation vapor pressure vs. temperature curve, P_a/K;

R_n net solar radiation, J/(mm^2·day);

ρ fluid mass density, g/mm^3;

c_p specific heat of air at constant pressure, J/(g·K);

$e_s(T)$ saturation vapor pressure at the temperature of the evaporation site, Pa;

e partial pressure of water vapor, Pa.

r_a the lumped atmospheric resistance over the 2m above the canopy top, day/mm;

r_c the lumped resistance to flow through the canopy which does not vary with water supply, day/mm;

γ_o the surface psychrometric constant, Pa/K.

When the stomas fully open, the canopy transpiration rate E_v will reach its maximum value – potential canopy transpiration E_{pv}, thus making k_v to be its maximum value as well, which is called the potential canopy conductance k_v^*:

$$k_v^* = \frac{E_{pv}}{E_{ps}} = \frac{1 + \Delta/\gamma_0}{1 + \Delta/\gamma_0 + (1-M)\left(\frac{r_c}{r_a}\right)_{M\to 0} + M\left(\frac{r_c}{r_a}\right)_{M=1}} \tag{5}$$

where $(r_c/r_a)_{M\to 0}$ is the resistance ratio for open canopies, which is related to the exponent relating shear stress on foliage to horizontal wind velocity and horizontal leaf area index. $(r_c/r_a)_{M=1}$ is the resistance ratio for closed (M=1) canopies whose mainly influence factor is the ratio of stem height h_s and tree height h. According to the Eq. (5) and explanations above, the resistance ratio can be fixed once the vegetation specie is given. The potential canopy conductance k_v^* is inversely proportion to the canopy cover M. The k_v^*-M curve is called water demand curve.

The relationship between k_v^* and M can also be described by water balance equation. In the growing season, the average inflows and outflows of the soil column can be described as:

$$P_\tau - m_v E[E_r] - \Delta S = m_v E[R_{sj}] + E[E_{T\tau}] + m_\tau v - m_\tau w \tag{6}$$

where

P_τ growing season precipitation, mm;

m_v the number of independent storm times, dimensionless;

E_r the storm surface retention depth, mm

R_{sj} storm rainfall excess, mm

ΔS average carryover (from dormant season to growing season) soil moisture storage, mm;

m_τ the growing season length, day;

v percolation to water table, mm/day;

w capillary rise from water table, mm/day;

E[ ]   means the expected value of [ ].

Some assumptions are made to describe each item (Eagleson 1978a, b, c, d, e, f, g). Thus, the water balance of the growing season can be expressed as:

$$Mk_v^* = \frac{V_e}{m_{tb}E_{ps}} \tag{7}$$

5 where Ve is the volume of soil moisture (per unit of surface area) available for exchange with atmosphere during average interstorm period (mm), m_{tb} is mean time between storms (h), more detail can be found in the appendix.

Equation (7) describes water supply in naturally selected canopy moisture state, while Eq. (5) describes water demand of fixed vegetation species. By drawing these two lines in a figure (Fig. 2), we can notice that the water demand grows with the increase of M, but as water is limited, water supply decreases under M enhancement. The intersection point of these two lines is the

10 theoretical optimal canopy cover and potential canopy conductance in the vegetation state-space. This method is applied in each grid (10km x 10km) of NECT area, and the input values are listed in Table 1. The input data and parameters include remote sensing data, meteorological data, vegetation data and soil data. The remote sensing data are the vegetation cover and *LAI*. The main meteorological data are length of growing season, potential evaporation, air temperature and storm duration. The main vegetation data are surface retention depth, leaf angle and stem height. The main soil data are soil porosity and

15 hydraulic conductivities.

4 Results and discussion

4.1 Canopy cover of NECT

The observed canopy cover M shows a significant gradient ranging from 1 in the east forests to 0 in the west desert (Fig. 3a). The dark blue area is mainly the forests of Changbai Mountains, where the average canopy cover reaches up to 0.83. The light

20 blue area is the Songnen Plain. Songnen Plain is one of the most famous commodity grain bases, rich in corn, sorghum, soybean, wheat and paddies (Zhou and Wang, 2003), with the average canopy cover of 0.55. Farther westward, there is Horqin Sand, in which most of the vegetation is grass. Then there is a narrow northeast-southwest-oriented band with relatively higher value (blue color) at around 120°E, which is mainly caused by the elevation. The band is the location of Greater Khingan Mountains. The east slope of the Greater Khingan Range is very steep, thus the maritime monsoon can bring a lot of rainfall, causing the

25 existence of forest ecosystem. However, most of the vegetation on the west slope is grass, mainly because of the gentle gradient and dry climate (Guo and Zhang, 2013). The grassland is Inner Mongolia steppe.

The Ecohydrological optimality theory is applied in this study to simulate theoretic optimal canopy cover (M^*) of NECT. As shown in Fig. 3b, the modeled canopy cover has the same trend with the actual M but transits more smoothly, which is mainly caused by the interpolation of meteorological data. The blank grids in the simulation result are due to the missing data of *LAI*.

30 The result indicates that the average M^* fits the average M well (for forest, $M^* = 0.822$ while $M = 0.826$; for grassland, $M^* = 0.353$ while $M = 0.352$; the correlation coefficient between M and M^* is 0.81). The corresponding areas are highlighted in

the figure of spatial distribution of ΔM, defined as M^* minus M (Fig. 3c). The spatial average ΔM is only -0.050 for the whole NECT area, meanwhile, there are 45.7% pixels of NECT area where ΔM value is between -0.1 to 0.1. There are three regions where the differences between M and M^* are relatively large. Region 1 is Yanbian Korean Autonomous Prefecture. The simulation result is relatively small mainly because of forest protection project. The Natural Forest Protection Project (NFPP) has been conducted in Northeastern China since 1998, aiming at protecting the natural forest resources (Wei et al., 2014). Yanbian forest acreage has increased by 800 km^2 during the first stage of NFPP. The dark red area is Hunchun City. Hunchun is a representative nature reserve, and the forest acreage has increased by 9,009 ha during 1999 to 2012 (Li, 2014). Region 2 is the southern Xilin Gol Grassland. In the past decades, Xilin Gol Grassland is extremely dry and had been suffering from severe degradation (Tong et al, 2002). The Beijing-Tianjin Sand Source Control Project is undertaken to improve the canopy cover of degraded grassland. Over 66,000 water source projects and 47,000 water saving irrigation projects increased the water supply of this area, thus contributing to the increase of vegetation activities (Yu et al, 2010). The irrigation part is not considered in the Eagleson's water balance system, which leads to the deviation of the modeled results. In the crop region (the blue frame in Fig. 3c), some M^* are higher than M while some are lower. This is because of the close relationship between canopy cover and crop growth stage. The growth process of various crops are different, and the timing of plantation and harvesting are mainly affected by human intervention rather than natural processes (Liu et al, 2013; Kim and Wang, 2005). Meanwhile, the water supply for the crop is not only from natural hydrological cycle but also from agricultural irrigation, which is not considered in the theory.

The correlation coefficient R between M and M^* is high, which indicates the Ecohydrological Optimality theory is applied well in NECT during long-term period. Previous studies suggest there are lagged relationship between NDVI and climate factors, and the time lags are different at different regions or different biomes (Braswell et al., 1997; Piao et al., 2003; Li et al., 2011; Hu et al., 2011; Bao et al., 2015). Fig. 4 shows that in grassland area, the variation amplitude of M is smaller than M^*, the delay usually happens within a year; while in forest area, there is a trend delay across the years. For example, the M^* is increasing from 2007 to 2009, but the increasing trend of M does not appear until 2009 to 2010. This can be explained by the vegetation adaptation strategy to climate changes. For example, the canopy cover might not increase immediately with the increasing precipitation but might increase in next year. Eagleson's Theory describes how vegetation adapt to climate change in a relatively long term (Eagleson, 2002). Once climate changes, it takes years for vegetation to reach its optimum canopy cover.

4.2 Water balance components

As NECT is spanning a wide range from west to east, and the vegetation and climate vary significantly, the NECT is divided into three parts according to land cover types: forests, cropland and grassland (Ni and Zhang, 2000). The proportions of the water balance components for annual average growing season are calculated for each part based on Equation 6, as shown in Table 2. According to the researches conducted before, in grassland area, the interception was 20.86% and 7.88% for shrub and grass respectively (Peng et al, 2014), and the runoff of Xilin Gol grassland occupies around 0.046%~1.8% (Wang, 2008;

Miao, 2008). In forest area, the dominant tree species are Pinus koraiensis (Pk), Quercus mongolica (Qm), Populus davidiana (Pd) and B. platyphylla (Bp) (Chen, 2001; Zhang and Zhou, 2009). The interception consists 19.61% for Pk and 14.97% for Bp in Great Greater Khingan Mountains, and 10.20% for Pk in Changbai Mountains (Cai et al, 2006; Wang et al, 2006). The runoff coefficient of Suifen River and Secondary Songhua River are around 20%~30%, both of which are located in forest area (Huang, 1999; Song, 2010). The simulated interception and runoff for both grassland and forest area are consistent with previous studies, which demonstrates the reasonability of this theory. The negative value of ΔS in forest area means a recharge of soil moisture. As the air temperature in the non-growing season is low, most of the precipitation is snow rather than rain, so the water is frozen in the soil and melts in the next spring (Fan et al, 2006; Yang et al, 2006). Therefore, most of the water is stored in the dormant season for the vegetation grow in the next growing season.

The rationality of the calculated proportions of water balance components for each part demonstrates the applicability of the optimality theory. By adapting this method, it is much easier to figure out the allocation of precipitation if the vegetation and soil conditions are known.

4.3 Sensitivity of M^* to vegetation properties

LAI, β and h_s/h control the physical and biological processes of plant canopies, such as interception and evaporation (Chen and Black, 1992; Asner, 1998; Huete et al. 2002). β and LAI are the dominant parameters for the interception calculation, thus leading to the variance of water supply for vegetation growth. β and h_s/h affect the plant evaporation through affecting the resistance ratio, which influences the water demand curve (Eagleson, 2002). The thresholds of the three parameters are from the experiments conducted before (Du, 2004; Wang et al, 2008; Rauner, 1976; Eagleson, 2002). Fig. 5 shows the different reactions of optimal canopy cover to vegetation species change between grassland and forest area. M^* increases with the increase of leaf angle and decrease of stem fraction and LAI. Mo (2015) studied the relationship between vegetation properties and optimal canopy cover in Horqin Sands, China, and got the same conclusion. In grassland area, the water demand curve is more sensitive to the variation of h_s/h compared to β. M^* decreases by 0.037 as h_s/h increases 0.10. The water supply curve changes a lot with the change of LAI, but slightly with β or h_s/h. In forest area, M^* is less sensitive to h_s/h than β or LAI. Because the average stem fraction of trees (0.4~0.5) is usually larger than grasslands or shrub (0.0~0.1), the water demand curve is much gentler (Eagleson, 2002), and changes little with h_s/h. The forest interception consists 14.24% of precipitation during growing season, which is larger than that of grassland. M^* increases by 0.108 and 0.094 with the 0.56 decrease of β and 2.45 of LAI, respectively (Table 3).

The sensitivity of M^* to vegetation properties can be used to offer advices about species choice and plant density to eco-restoration projects. If the purpose is to increase canopy cover, different strategies should be conducted in different area. For grassland area, shrubby or herbaceous plants with low h_s/h value are more welcome. Nevertheless, in forest area, as h_s/h does not affect canopy cover that much, more considerations should be taken into choosing the species with relatively lower β and LAI values. However, vegetation with a larger canopy cover always requires more water to maintain functions (Woodward

and Mckee, 1991; Zhang and Zhou, 2011). If the plant species are determined, the optimum canopy cover can be calculated, and the upper limit for plant density can be estimated.

4.4 Sensitivity of M^* to climate factors

Studies of relationship between climate factors and vegetation growth condition reveal that precipitation and temperature are the two dominant factors that affect M^* (Ichii et al, 2002; Liu et al, 2015). Under this framework, the variation of precipitation (P_τ) affects the availability of water, thus changing water supply curve; air temperature (t_a) affects not only water supply but also water demand, through changing resistance ratio and evaporation (Fig. 6). In grassland area, M^* exhibits a positive relationship with precipitation but a negative relationship with air temperature (Fig. 6(a)(b)), of which is consistent with studies conducted before (He et al, 2015; Peng et al, 2012). This can be explained by the limited water supply in arid and semi-arid regions, and that the increase of air temperature enhances transpiration and evaporation intensity (Duan et al, 2011; Mao et al, 2012). The variation of grassland M^* during 2000-2013 (Fig. 4(a)) also shows a similar trend of M^* and precipitation, while the trend of air temperature is different from that of precipitation in most years. In forest area, M^* increases with the increase of precipitation and decrease of air temperature, but the variance of grassland M^* is less than that of forest with the same range of air temperature, which indicates the forest plants are more sensitive to air temperature than grassland. However, the result is different from previous studies. Most correlation analysis of NDVI with air temperature and precipitation shows that in forest area, NDVI increases with the increase of air temperature and decrease of precipitation, because air temperature is the dominant factor in humid areas, and the light use efficiency increases under elevated air temperatures (Peng et al, 2012; Wang et al, 2014; Liu et al, 2011). The difference may be caused by the deficient hypotheses of the theory. Under this framework, the surface runoff is assumed to be Hortonian, but in most humid areas, the runoff is saturation excess. The improper hypothetical runoff mechanism leads to the deviation of runoff in water-sufficient areas, thus causing the deviation of water supply curve.

5 Conclusion

In this study, remote-sensed NDVI is used to generate actual canopy cover of NECT, while the ecohydrological optimality method has been applied to calculate the optimal canopy cover. The proportions of water balance components have been explored, as well as the influence of vegetation properties and climate factors on optimal canopy cover. Main conclusions are summarized as follows:

(1) The observed canopy cover M shows a significant decreasing gradient from east forests to west. The modeled canopy cover M^* has the same trend with M but transits more smoothly, which is mainly caused by the interpolation of meteorological data. The relatively lower M^* in Yanbian Korean Autonomous Prefecture and Xilin Gol Grassland is mainly because of human activity. The correlation coefficient R between M and M^* is 0.81, which indicates the Ecohydrological Optimality theory is

applied well in NECT during long-term period. There is a two-year-lag between $M*$ and M during 2002-2012, due to the long-term adaptation strategy of vegetation to climate change.

(2) The proportions of the water balance components are calculated for three parts: forest, cropland and grassland. The simulated results are within the observed range, which demonstrates the reasonability of this theory. By adapting this method, it is much easier to figure out the allocation of precipitation with fixed vegetation and soil conditions.

(3) $M*$ has the positive relationship with β and negative relationship with h_s/h and LAI. Grassland plants are more sensitive to h_s/h and LAI compared to β, while forest plants are more sensitive to β and LAI than h_s/h. The sensitivity of $M*$ to vegetation properties can be used to offer advices about species choice and plant density to eco-restoration projects.

(4) Precipitation and temperature are the two dominant climate factors that affect $M*$. $M*$ increases with the increase of precipitation and decrease of air temperature. Eagleson's ecohydrological optimality theory offers an opportunity to explore the quantitative relation between vegetation and climate factors from the mechanism, but the runoff mechanism description in wet region still needs improvement.

Acknowledgement

This work was supported by National Natural Science Foundation (No. 51479088, 41630856).

Appendix

Algorithm of optimal canopy cover

Eagleson made several assumptions for each item of Eq. (4). Poisson precipitation model was used to simulate the precipitation process by random storm depth and duration (Eagleson, 1978b). The probability density functions of storm depth and storm duration are incomplete gamma and exponential distribution, respectively. The growing season precipitation can be expressed as:

$$P_\tau = m_v/m_h \tag{A.1}$$

where m_h is the mean storm depth, mm.

Surface retention $m_v E_r$ is the water held on the surface during the rainstorm of duration. The total surface retention is proportioned by bare soil and vegetation canopy:

$$E[E_r] = (1 - M)E[E_{rs}] + ME[E_{rv}] \tag{A.2}$$

where E_{rs} and E_{rv} are the surface retention loss of bare soil and vegetation canopy, and can be further expressed as:

$$E[E_r] = (1 + M\eta_0\beta L_t)h_0 = \overline{h_0} \tag{A.3}$$

where η_o is the ratio of stomated leaf area to illuminated leaf area, dimensionless; β is the cosine of leaf angle, dimensionless; L_t is the foliage area index, dimensionless; h_o is the surface retention depth, mm. The interception depth retained on the horizontal projection of leaves is assumed to be 1.00 cm (Eagleson, 1978d).

Average carryover soil moisture storage ΔS (mm) is determined by the soil profile and seasonality (Eagleson, 2002):

$$\Delta S = -\left[P_d - (1 - M)E_{psd}m_d - Y_d\right] \tag{A.4}$$

where P_d (mm), E_{psd} (mm/day), m_d (day), and Y_d (day) are the precipitation, evaporation, days and runoff in the non-growing season, respectively.

5   Assume that there is no surface inflow from outside of the region, and the surface runoff is Hortonian (Eagleson, 1978e). When the storm intensity m_i and storm duration m_{tr} are independent random variables, the storm surface runoff $m_v R_{sj}$ is:

$$E(R_{sj}) = m_h e^{-G - 2\sigma^{3/2}} \tag{A.5}$$

where

$$G \equiv \omega K(1)\left(\frac{1 + s_0^c}{2}\right) \tag{A.6}$$

10    $$\sigma \equiv \left[\frac{5n_e\lambda_0^2 K(1)\psi(1)(1 - s_0)^2 \phi_i(d, s_0)}{6\pi\delta m\kappa_0^2}\right] \tag{A.7}$$

where

s_o space-time average soil moisture in the root zone, dimensionless;

ω $= 1/m_i$;

$K(1)$ effective saturated hydraulic conductivity of soil, cm day^{-1};

15   n_e effective soil porosity, dimensionless;

λ_0 scale parameter of probability density function of storm depth, cm^{-1};

$\psi(1)$ saturated matrix potential of soil, cm;

ϕ_i sorption diffusivity, dimensionless;

δ $= 1/m_{tr}$, day^{-1};

20   m soil pore size distribution index, dimensionless;

κ_o shape parameter or distribution index of storm depth, dimensionless.

Evapotranspiration consists of bare soil evaporation and vegetal transpiration:

$$E[E_{T\tau}] = m_v m_{tb} E_{ps\tau}\left[(1 - M)\beta_s + Mk_v^*\beta_v\right] \tag{A.8}$$

where m_{tb} is the mean time between storms, day; $E_{ps\tau}$ is the potential free water surface potential evaporation during growing

25   season, mm/day; β_s and β_v are the bare soil evaporation efficiency and canopy transpiration efficiency respectively (Eagleson, 1978d).

The percolation rate is mainly affected by s_o (Eagleson, 1978f):

$$v(s_0) = K(1)s_0^c \tag{A.9}$$

The capillary rise is considered to be 0 due to the deep water table in NECT.

30   Using Eq. (A.1)~(A.9), Eq. (4) gives the water balance of growing season as:

$$1 - e^{-G - 2\sigma^{3/2}} - \frac{\overline{h_0}}{m_h} + \frac{\Delta S}{m_v m_h} = \frac{m_{tb} E_{ps}}{m_h} [(1 - M)\beta_s + M k_v^* \beta_v] + \frac{m_\tau K(1)}{P_\tau} s_0^c$$

(A.10)β_v is equal to 1.0 when the water condition reaches optimal state. When the bare soil evaporation is ignored, Eq. (A.10) can be simplified into

$$Mk_v^* = \frac{V_e}{m_{tb} E_{ps}} \tag{A.11}$$

5 where, $V_e = m_h - m_h e^{-G - 2\sigma^{3/2}} - \overline{h_0} + \frac{\Delta S}{m_v} - \frac{m_\tau K(1)}{m_v} s_0^c$ (A.12)

Reference

Allen, R. G. Crop evapotranspiration: guidelines for computing crop water requirements [M], xxvi, 300 p. pp., Food and Agriculture Organization of the United Nations, 1998, Rome.

Asner G P. Biophysical and Biochemical Sources of Variability in Canopy Reflectance[J]. Remote Sensing of Environment,
10 1998, volume 64(98):234-253(20).

Austin A T, Sala O E. Carbon and nitrogen dynamics across a natural precipitation gradient in Patagonia, Argentina[J]. Journal of Vegetation Science, 2002, 13(3):351-360.

Bao G, Bao Y, Sanjjava A, et al. NDVI-indicated long-term vegetation dynamics in Mongolia and their response to climate change at biome scale[J]. International Journal of Climatology, 2015, 35(14):4293–4306.

15 Baret F, Clevers J G P W, M.D. Steven. The robustness of canopy gap fraction estimates from red and near-infrared reflectances: A comparison of approaches[J]. Remote Sensing of Environment, 1995, 54(2):141-151.

Braswell B H, Schimel D S, Linder E, et al. The Response of Global Terrestrial Ecosystems to Interannual Temperature Variability[J]. Science, 1997, 278(278):870-873.

Cai T, Zhu D, Sheng H. Rainfall redistribution in virgin Pinus koaiensis forest and secondary Betual platyphylla forest in
20 Northeast China[J]. Science of Soil & Water Conservation, 2006. (in Chinese)

Canadell JG, Steffen WL, White PS. IGBP/GCTE terrestrial transects: dynamics of terrestrial ecosystems under environmental change—introduction[J]. Journal of Vegetation Science, 2002, 13:298–300

Carlson T N, Ripley D A. On the relation between NDVI, fractional vegetation cover, and leaf area index ☆[J]. Remote Sensing of Environment, 1997, 62(3):241-252.

25 Chen J. M, Black T. A. Defining leaf area index for non‐flat leaves[J]. Plant, Cell & Environment, 1992, 15(4):421-429.

Chen X. Change of tree diversity on Northeast China Transect (NECT)[J]. Biodiversity & Conservation, 2001, 10(7):1087-1096.

Dorman M, Svoray T, Perevolotsky A. Homogenization in forest performance across an environmental gradient – The interplay between rainfall and topographic aspect[J]. Forest Ecology & Management, 2013, 310(1):256-266.

Du J. Approach to the Phenotypic Plasticity of Leymus chinensis Population Responding to Grazing[D]. Northeast Normal University, 2004. (in Chinese)

Duan H C, Yan C Z, Tsunekawa A, et al. Assessing vegetation dynamics in the Three-North Shelter Forest region of China using AVHRR NDVI data (SCI)[J]. Environmental Earth Sciences, 2011, 64(4):1011-1020.

5   Eagleson P S, Tellers T E. Ecological optimality in water-limited natural soil-vegetation systems: 2. Tests and applications[J]. Water Resources Research, 1982, 18(2):341–354.

Eagleson P S. Climate, soil, and vegetation: 1. Introduction to water balance dynamics[J]. Water Resources Research, 1978(a), 14(5):705–712.

Eagleson P S. Climate, soil, and vegetation: 2. The distribution of annual precipitation derived from observed storm

10   sequences[J]. Water Resources Research, 1978(b), 14(5):713–721.

Eagleson P S. Climate, soil, and vegetation: 3. A simplified model of soil moisture movement in the liquid phase[J]. Water Resources Research, 1978(c), 14(5):722-730.

Eagleson P S. Climate, soil, and vegetation: 4. The expected value of annual evapotranspiration[J]. Water Resources Research, 1978(d), 14(5):731–739.

15   Eagleson P S. Climate, soil, and vegetation: 4. The expected value of annual evapotranspiration[J]. Water Resources Research, 1978, 14(5):731–739.

Eagleson P S. Climate, soil, and vegetation: 5. A derived distribution of storm surface runoff [J]. Water Resources Research, 1978(e), 14(5):741–748.

Eagleson P S. Climate, soil, and vegetation: 6. Dynamics of the annual water balance[J]. Water Resources Research, 1978(f),

20   14(5):749–764.

Eagleson P S. Climate, soil, and vegetation: 7. A derived distribution of annual water yield[J]. Water Resources Research, 1978(g), 14(14):765–776.

Eagleson P S. Ecohydrology: Darwinian expression of vegetation form and function[M]. Cambridge University Press, 2002.

Eagleson P S. Ecological optimality in water-limited natural soil-vegetation systems: 1. Theory and hypothesis[J]. Water

25   Resources Research, 1982, 18(2):325-340.

Fan S X, Gao Y, Cheng Y C, et al. RESEARCH OF PLOT TESTING FOR EFFECTS OF THE WOODS AND GRASS VEGETATION ON RUNOFF[J]. Journal of Shandong Agricultural University, 2006, 37(1):43-47. (in Chinese)

Fontana F, Rixen C, Jonas T, et al. Alpine Grassland Phenology as Seen in AVHRR, VEGETATION, and MODIS NDVI Time Series - a Comparison with In Situ Measurements[J]. Sensors, 2008, 8(4):2833-2853.

30   Füssler J S, Gassmann F. On the role of dynamic atmosphere–vegetation interactions under increasing radiative forcing[J]. Global Ecology & Biogeography, 2000, 9(4):337–349.

Graetz R D. The nature and significance of the feedback of changes in terrestrial vegetation on global atmospheric and climatic change[J]. Climatic Change, 1991, 18(2-3):147-173.

Guo X Y, Zhang H Y. The Vegetation Dynamic Research Under of Eco-geographical Region Framework on Greater Khingan Mountains[J]. Scientia Geographica Sinica, 2013, 33(2):181-188. (in Chinese)

Gutman G, Ignatov A. The derivation of the green vegetation fraction from NOAA/AVHRR data for use in numerical weather prediction models[J]. International Journal of Remote Sensing, 1998, 19(8):1533-1543.

5   Hatton T. J, Salvucci G. D, Wu H. I. Eagleson's optimality theory of an ecohydrologcal equilibrium: quo vadis?[J]. Functional Ecology, 1997, 11(6):665-674.

He B, Chen A, Wang H, et al. Dynamic Response of Satellite-Derived Vegetation Growth to Climate Change in the Three North Shelter Forest Region in China[J]. Remote Sensing, 2015, 7(7):9998-10016.

Hmimina G, Dufrêne E, Pontailler J Y, et al. Evaluation of the potential of MODIS satellite data to predict vegetation
10   phenology in different biomes: An investigation using ground-based NDVI measurements[J]. Remote Sensing of Environment, 2013, 132(6):145–158.

Hu M Q, Mao F, Sun H, et al. Study of normalized difference vegetation index variation and its correlation with climate factors in the three-river-source region[J]. International Journal of Applied Earth Observation & Geoinformation, 2011, 13(1):24-33.

Huang G. Impact of climate change on water resources of international rivers in northeastern China[J]. Acta Geographica
15   Sinica, 1999. (in Chinese)

Huete A, Didan K, Miura T, et al. Overview of the radiometric and biophysical performance of the MODIS vegetation indices[J]. Remote Sensing of Environment, 2002, 83(s 1–2):195-213.

Ichii K. Global correlation analysis for NDVI and climatic variables and NDVI trends: 1982-1990[J]. International Journal of Remote Sensing, 2002, 23(18):3873-3878.

20   J. Wang, P. M. Rich, K. P. Price. Temporal responses of NDVI to precipitation and temperature in the central Great Plains, USA[J]. International Journal of Remote Sensing, 2003, volume 24(11):2345-2364.

Jiang Z, Huete A R, Chen J, et al. Analysis of NDVI and scaled difference vegetation index retrievals of vegetation fraction[J]. Remote Sensing of Environment, 2006, 101(3):366-378.

Kerkhoff A J, Martens S N, Milne B T. An ecological evaluation of Eagleson's optimality hypotheses[J]. Functional Ecology,
25   2004, 18(3):404-413.

Kim Y, Wang G. Modeling seasonal vegetation variation and its validation against Moderate Resolution Imaging Spectroradiometer (MODIS) observations over North America[J]. Journal of Geophysical Research Atmospheres, 2005, 110(D7).

Koch G W, Scholes R J, Steffen W L, et al. The IGBP terrestrial transects: science plan[J]. Global Change Report, 1995(a).

30   Koch G W, Vitousek P M, Steffen W L, et al. Terrestrial transects for global change research[J]. Vegetatio, 1995(b), 121(1-2):53-65.

Li B, Tao S, Dawson R W. Relations between AVHRR NDVI and ecoclimatic parameters in China[J]. International Journal of Remote Sensing, 2002, 23(5):989-999.

Li S, Zhao Z, Wang Y, et al. Identifying spatial patterns of synchronization between NDVI and climatic determinants using joint recurrence plots[J]. Environmental Earth Sciences, 2011, 64(3):851-859.

Li X. Study on demonstration and construction of NFPP effect evaluation system in Yanbian Forest Region[D]. Northeast Forestry University, 2004 (in Chinese)

5 Liu C, Shang J, Vachon P W, et al. Multiyear Crop Monitoring Using Polarimetric RADARSAT-2 Data[J]. Geoscience & Remote Sensing IEEE Transactions on, 2013, 51(4):2227-2240.

Liu W, Cai T, Ju C, et al. Assessing vegetation dynamics and their relationships with climatic variability in Heilongjiang Province, northeast China[J]. Environmental Earth Sciences, 2011, 64(8):2013-2024.

Liu Y, Li Y, Li S, et al. Spatial and Temporal Patterns of Global NDVI Trends: Correlations with Climate and Human

10 Factors[J]. Remote Sensing, 2015, 7(10):13233-13250.

Liu Z, Notaro M. Assessing Global Vegetation-Climate Feedbacks from Observations[C]// AGU Fall Meeting Abstracts. AGU Fall Meeting Abstracts, 2005.

Lotsch A, Friedl M A, Anderson B T, et al. Coupled vegetation-precipitation variability observed from satellite and climate records[J]. Geophysical Research Letters, 2003, 30(14):107-218.

15 Mao D, Wang Z, Luo L, et al. Integrating AVHRR and MODIS data to monitor NDVI changes and their relationships with climatic parameters in Northeast China[J]. International Journal of Applied Earth Observation & Geoinformation, 2012, 18:528-536.

Mcpherson R A. A review of vegetation--atmosphere interactions and their influences on mesoscale phenomena[J]. Progress in Physical Geography, 2007, 31(3):261-285.

20 Miao B L, Liang C Z, Wang W, et al. Effects of vegetation on degradation surface runoff of typical steppe[J]. Journal of Soil and Water Conservation, 2008(2): 10-14. (in Chinese)

Mo K, Cong Z, Lei H. Optimal vegetation cover in the Horqin Sands, China[J]. Ecohydrology, 2015.

Myoung B, Choi Y S, Park S K. A review on vegetation models and applicability to climate simulations at regional scale[J]. Asia-Pacific Journal of Atmospheric Sciences, 2011, 47(5):463-475.

25 Ni J, Wang G. Northeast China transect (NECT): Ten--year synthesis and future challenges[J]. Acta Botanica Sinica, 2004, 46(4):379-391.

Ni J, Zhang X S. Climate variability, ecological gradient and the Northeast China Transect (NECT)[J]. Journal of Arid Environments, 2000, 46(3):313-325.

Nie Q, Xu J, Ji M, et al. The vegetation coverage dynamic coupling with climatic factors in Northeast China Transect.[J].

30 Environmental Management, 2012, 50(3):405-417.

Park H S, Sohn B J. Recent trends in changes of vegetation over East Asia coupled with temperature and rainfall variations[J]. Journal of Geophysical Research Atmospheres, 2010, 115(D14):1307-1314.

Peng H, Li X, Tong S. Effects of shrub (Caragana microphalla Lam.) encroachment on water redistribution and utilization in the typical steppe of Inner Mongolia[J]. Acta Ecologica Sinica, 2014, 34(9):2256-2265. (in Chinese)

Peng J, Dong W, Yuan W, et al. Responses of Grassland and Forest to Temperature and Precipitation Changes in Northeast China[J]. Advances in Atmospheric Sciences, 2012, 29(05):1063-1077.

Piao S, Fang J, Zhou L, et al. Interannual variations of monthly and seasonal normalized difference vegetation index (NDVI) in China from 1982 to 1999[J]. Journal of Geophysical Research Atmospheres, 2003, 108(D14):ACL 1-1.

5 Piao S, Mohammat A, Fang J, et al. NDVI-based increase in growth of temperate grasslands and its responses to climate changes in China[J]. Global Environmental Change, 2006, 16(4):340-348.

Piao S, Wang X, Ciais P, et al. Changes in satellite-derived vegetation growth trend in temperate and boreal Eurasia from 1982 to 2006[J]. Global Change Biology, 2011, 17(10):3228–3239.

Rauner, J.L., Vegetation and the Atmosphere, vol. 2, Case Studies, edited by J.L. Monteith, pp. 241–264, Academic Press,
10 New York, 1976.

Schultz P A, Halpert M S. Global correlation of temperature, NDVI and precipitation[J]. Advances in Space Research, 1993, 13(13):277-280.

Shao W, Yang D, Sun F, et al. Analyzing the Regional Soil-Vegetation-Atmosphere Interaction Using Both the Eagleson and Budyko's Water Balance Models[J]. Procedia Environmental Sciences, 2011, 10:1908-1913.

15 Song X. Precipitation, streamflow and sediment transport changes and its response to human activities in Songhua basin[D]. Graduate University of Chinese Academy of Sciences, 2010. (in Chinese)

Tong C, Wu J, Yong S, et al. A landscapescale assessment of steppe degradation in the Xilin River basin, Inner Mongolia, China[J]. Journal of Arid Environments, 2004, 59(1):133-149.

Wang A, Pei T, Jin C, et al. Estimation of rainfall interception by broad-leaved Korean pine forest in Changbai Mountains[J].
20 Chinese Journal of Applied Ecology, 2006, 17(8):1403-7. (in Chinese)

WANG Qiang, ZHANG Bo, ZHANG Zhiqiang, ZHANG Xifeng, DAI Shengpei. The Three-North Shelterbelt Program and Dynamic Changes in Vegetation Cover[J]. Journal of Resources and Ecology, 2014, 5(1):53-59.

Wang Y F, Xing-Guo M O, Hao Y B, et al. Simulating seasonal and interannual variations of ecosystem evapotranspiration and its components in Inner Mongolia steppe with VIP model[J]. Journal of Plant Ecology, 2008, 32(5):1052-1060. (in Chinese)

25 Wang Y, Yun W, Miao B, et al. The Pattern and Dynamics of Surface Runoff in the Typical Steppe of Inner Mongolia[J]. Research of Soil & Water Conservation, 2008, 15(4):114-115. (in Chinese)

Wei Y, Dapao Y U, Lewis B J, et al. Forest Carbon Storage and Tree Carbon Pool Dynamics under Natural Forest Protection Program in Northeastern China[J]. Chinese Geographical Science, 2014, 24(04):397-405.

Woodward F I, Mckee I F. Vegetation and climate[J]. Environment International, 1991, 17(6):535-546.

30 Yang H, Pei T, Guan D, et al. Soil moisture dynamics under broad-leaved Korean pine forest in Changbai Mountains[J]. The Journal of Applied Ecology, 2006, 17(4):1403-7. (in Chinese)

Yu X, Gu J, Yue Y, at al. Benefit evaluation on forestry ecological projects[M]. Science Press, 2010. (in Chinese)

Yuan X, Li L, Chen X, et al. Effects of Precipitation Intensity and Temperature on NDVI-Based Grass Change over Northern China during the Period from 1982 to 2011[J]. Remote Sensing, 2015, 7(8):10164-10183.

Zhang Y, Zhou G. Exploring the effects of water on vegetation change and net primary productivity along the IGBP Northeast China Transect[J]. Environmental Earth Sciences, 2011, 62(62):1481-1490.

Zhou G S. Global Ecology[M]. China Meteorological Press, 2003. (in Chinese)

Zhou L, Tucker C J, Kaufmann R K, et al. Variations in northern vegetation activity inferred from satellite data of vegetation index during 1981 to 1999[J]. Journal of Geophysical Research Atmospheres, 2001, 106(D17):20069-20083.

Table 1: The terminology, interpretation, units and values of inputs

	Terminology	Interpretation and units	Value
Remote Sensing Data	f_c	Average vegetation cover of growing season	0.00 ~ 1.00
	M_d	Average vegetation cover of non-growing season	0.00 ~ 1.00
	l_t	Leaf Area Index (LAI) in growing season, dimensionless	0.00 ~ 4.70
	l_{td}	Leaf Area Index (LAI) in dormant season, dimensionless	0.00 ~ 1.70
Meteorological Data	m_t	length of the growing season, days	153
	m_d	length of the non-growing season, days	212
	E_{pst}	free water surface potential evaporation during growing season, mm/d	3.6 ~ 4.4
	E_{psd}	free water surface potential evaporation during dormant season, mm/d	0.7 ~ 1.0
	P_τ	precipitation in growing season, mm	149.7 ~ 624.3
	P_d	precipitation in dormant season, mm	26.2 ~ 226.3
	t_0	average temperature in growing season, ℃	16.12 ~ 21.24
	m_{tb}	mean time between storms, days	4.65 ~ 6.35
	m_{tr}	mean storm duration, days	0.37 ~ 0.64
	γ_0	surface psychrometric constant, Pa/K	0.06
Vegetation Data	m	exponent relating shear stress on foliage to horizontal wind velocity, dimensionless	0.5
	n	number of sides of each foliage element producing surface resistance to wind, dimensionless	2
	η_0	stomated leaf area / illuminated leaf area, dimensionless	2.50
	h_0	surface retention depth, mm	1.00
	β	cosine of leaf angle, dimensionless	0.45
Soil Data	h_s	stem height (i.e., height of crown base above substrate), m	
	h	height of tree from ground surface to top of crown, m	
	m	soil pore size distribution index, dimensionless	0.50
	n_e	effective soil porosity, dimensionless	0.45
	d	diffusivity index of soil, dimensionless	4.30
	ψ	saturated matrix potential of soil, mm	900.0
	k	effective saturated hydraulic conductivity of soil, mm/d	29.4
	s_0	space-time average soil moisture concentration in the root zone, dimensionless	0.30 ~ 0.62

Table 2. Water balance components of different land cover types

		grassland		cropland		forests	
result	M	0.352		0.548		0.826	
	M^*	0.353		0.557		0.822	
		mm	/P	mm	/P	mm	/P
Water balance component	*Precipitation*	253	100.00%	414	100.00%	478	100.00%
	Interception	29	11.61%	39	9.29%	68	14.24%
	Runoff	1	0.19%	119	28.77%	119	24.92%
	ΔS	91	36.29%	14	3.34%	-74	-15.47%
	Evaporation	131	51.90%	243	58.60%	365	76.31%

5   **Table 3: The variance of inputs and their corresponding *M***

inputs	variation range	Grassland M^*	Forest M^*
β	0.01~0.57	0.346~0.358	0.755~0.863
LAI	0.10~2.55	0.313~0.357	0.770~0.864
h_s/h	0.00~0.10 (grassland); 0.35~0.45(forest)	0.317~0.354	0.817~0.827
P_t	24.26~26.26 (grassland); 46.83~48.83(forest)	0.330~0.377	0.800~0.844
t_a	18.08~20.08(grassland); 17.09~19.09(forest)	0.333~0.371	0.783~0.841
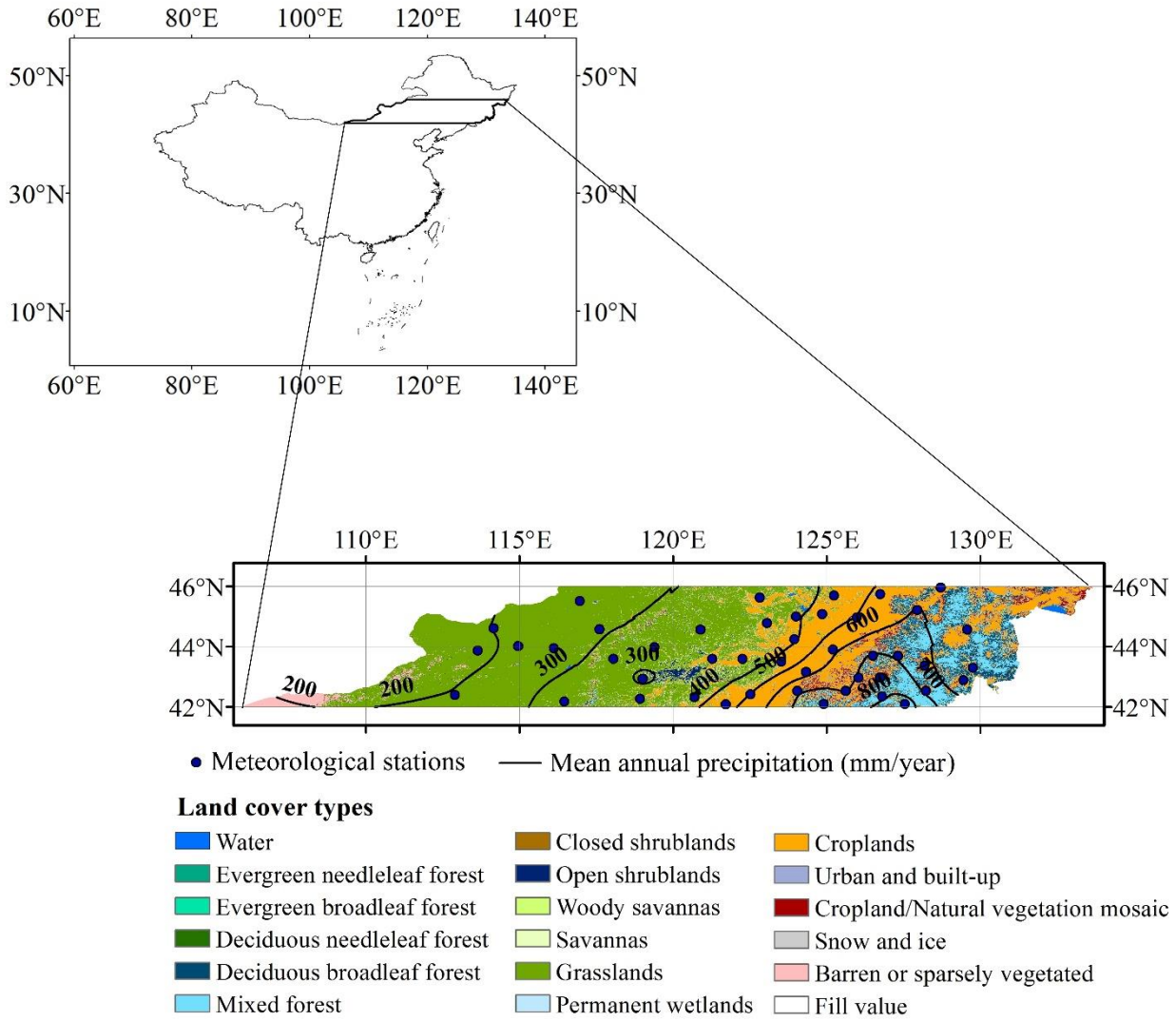
Figure 1: The geographic location, land cover, spatial distribution of precipitation and meteorological stations locations of NECT.
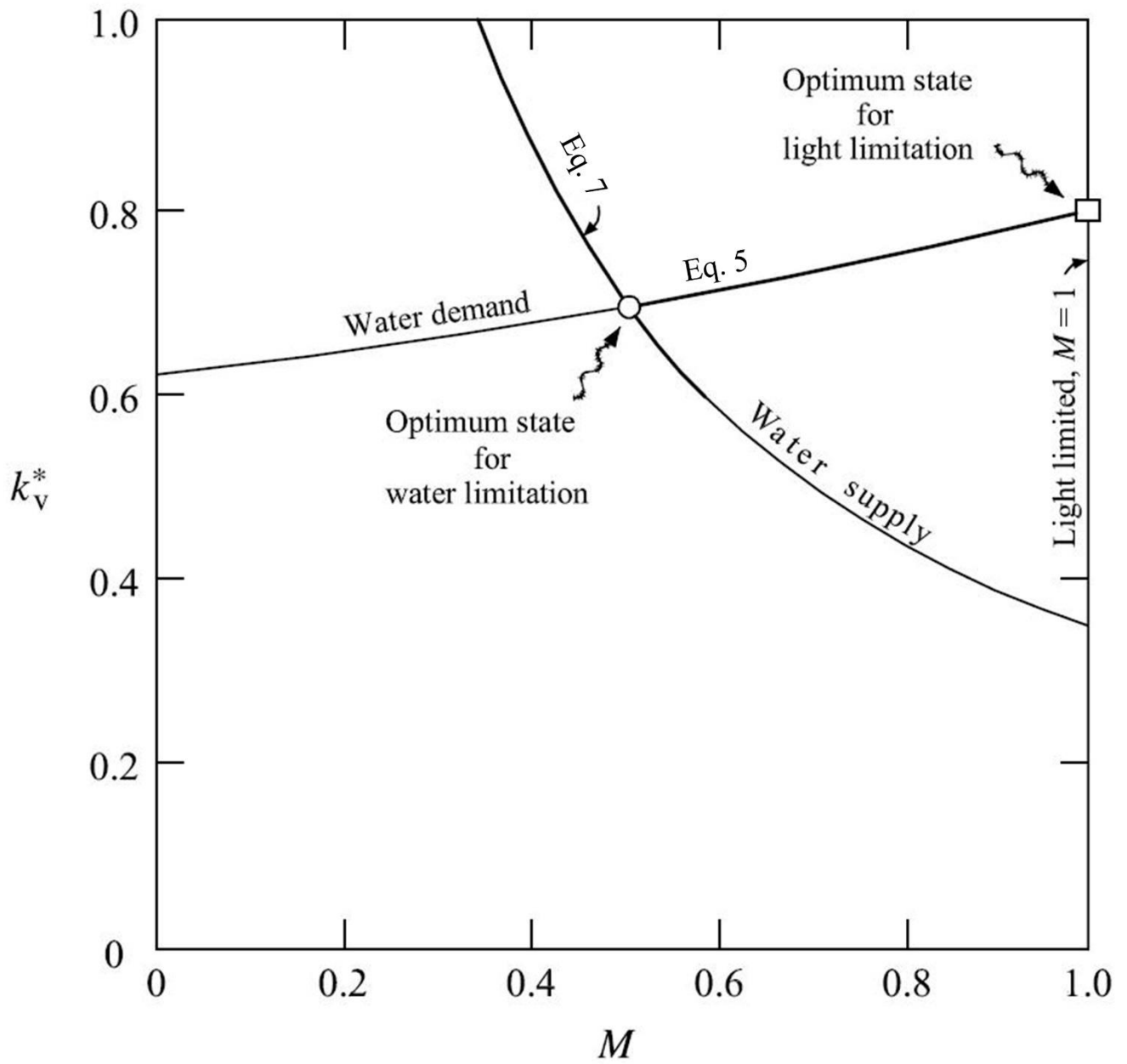
Figure 2: Optimum canopy state (from Eagleson, 2002).
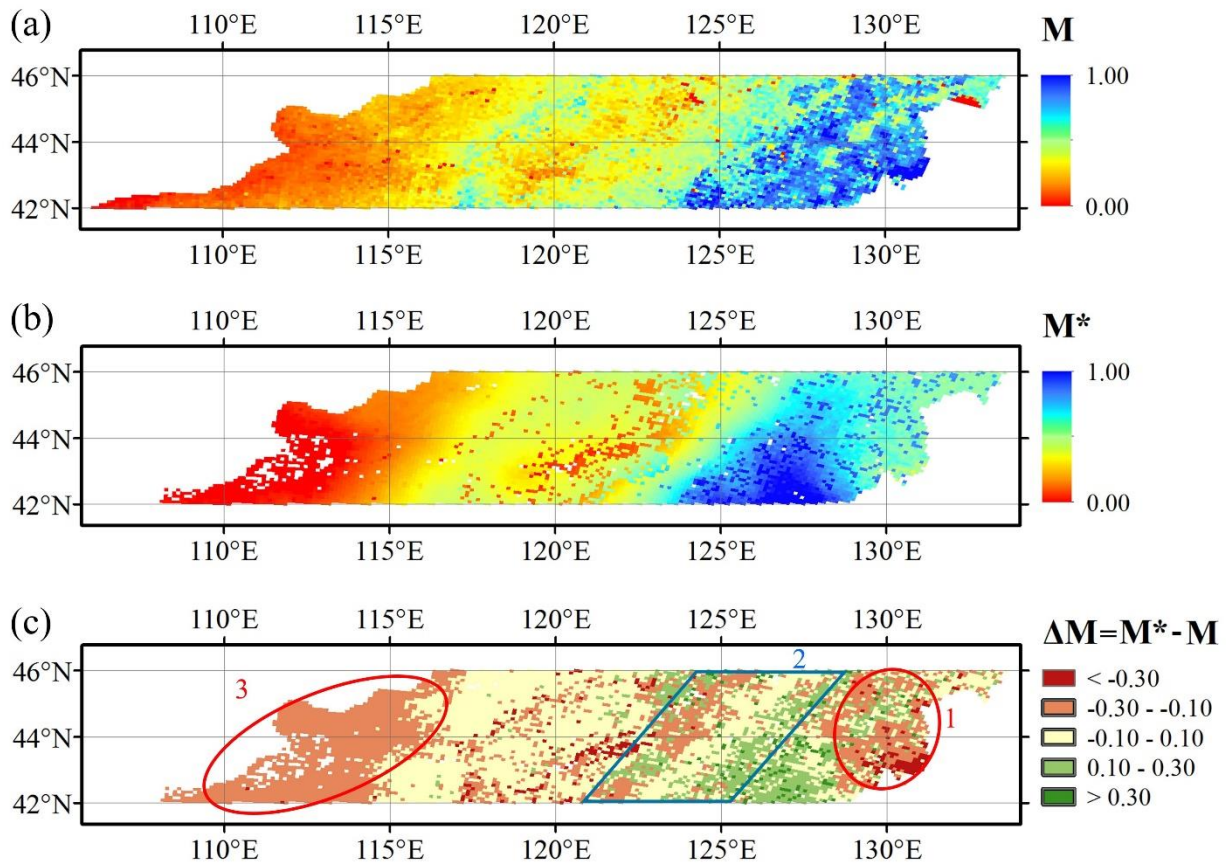
Figure 3: Spatial distribution of mean canopy cover from MODISdata, optimal canopy cover and their differences.
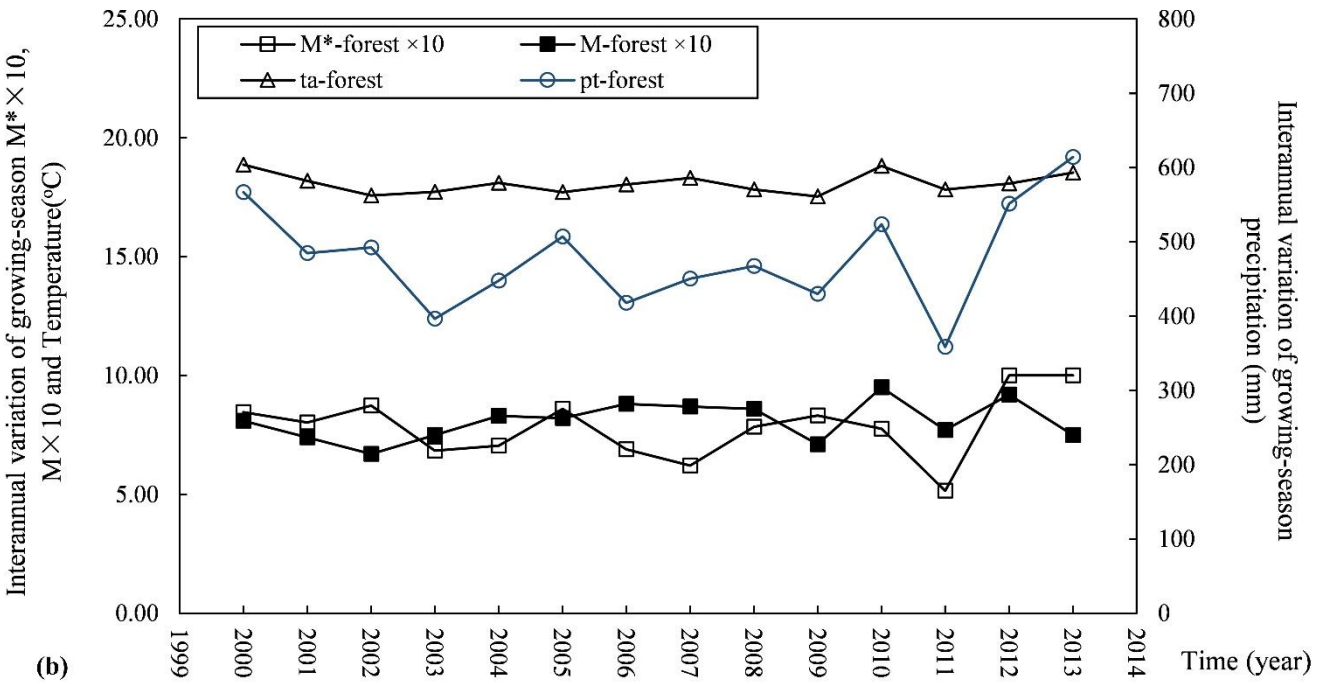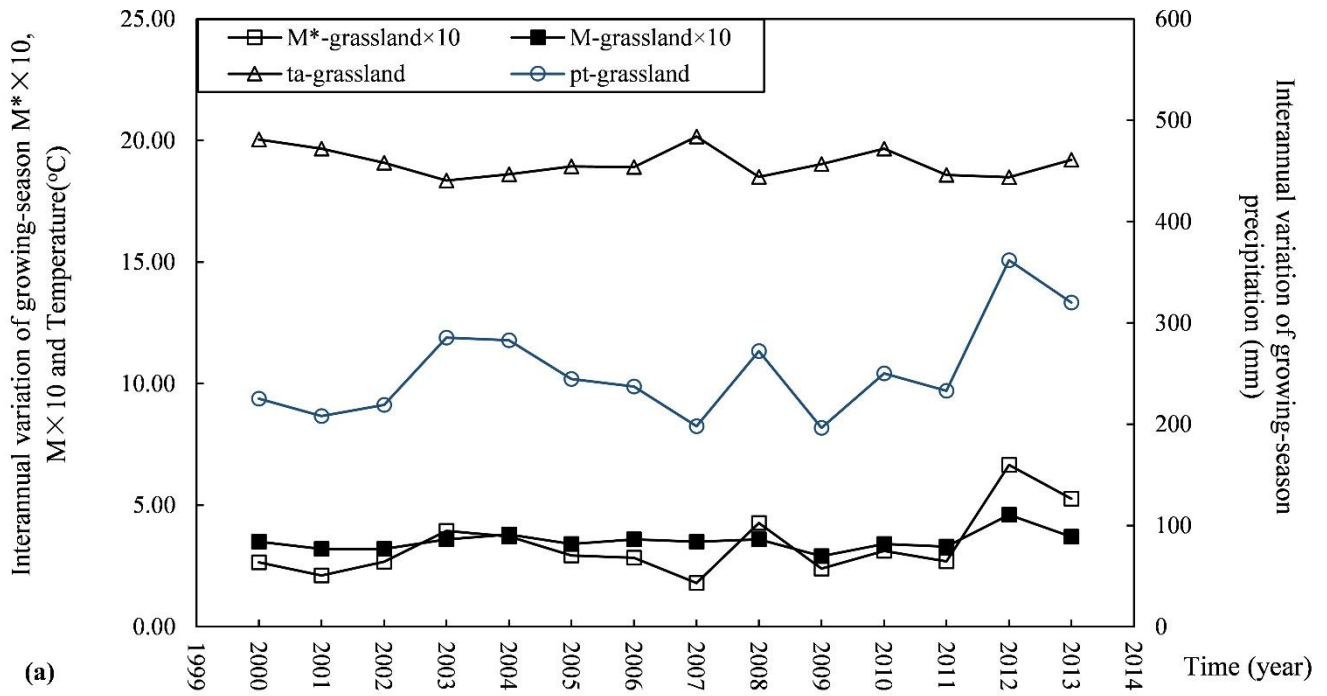
Figure 4: Variation of *M** , *M* precipitation (*P_τ*) and air temperature (*t_a*) during 2000-2013 ((a) grassland; (b) forest).
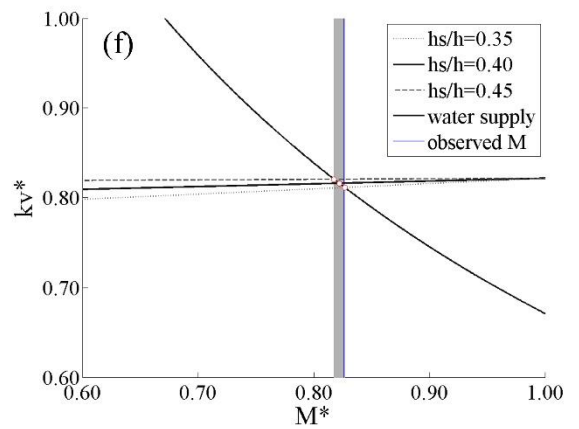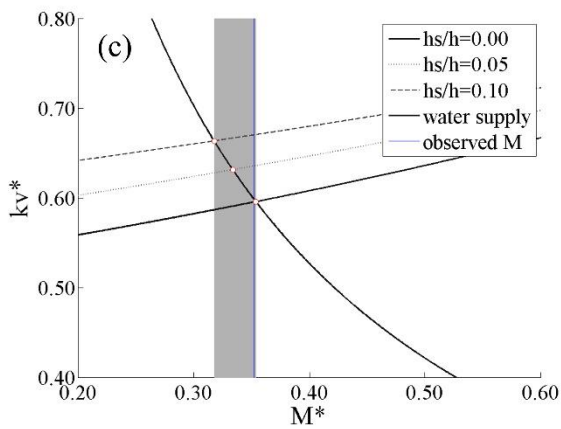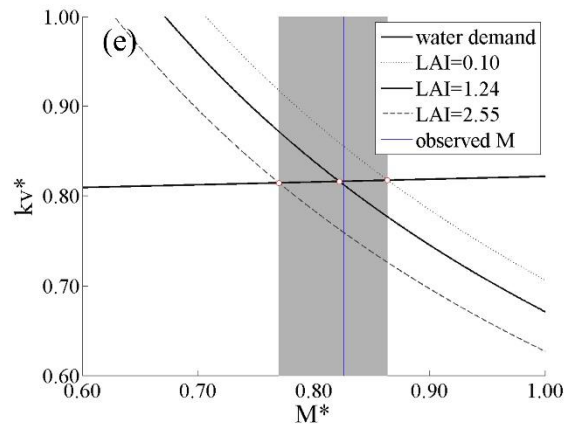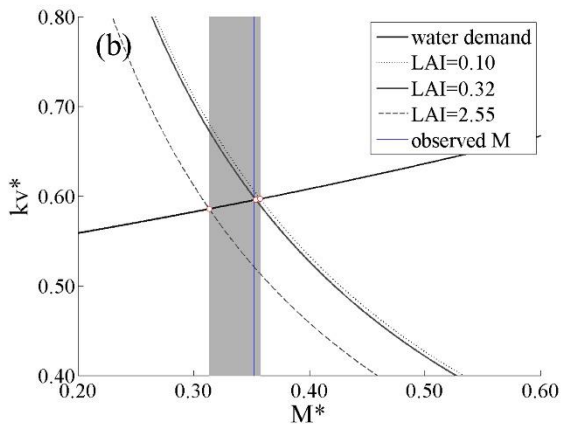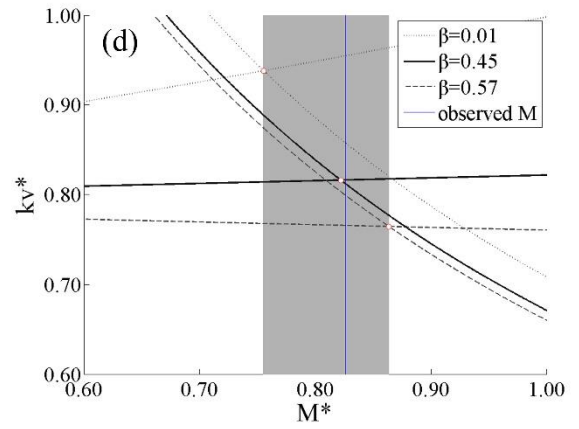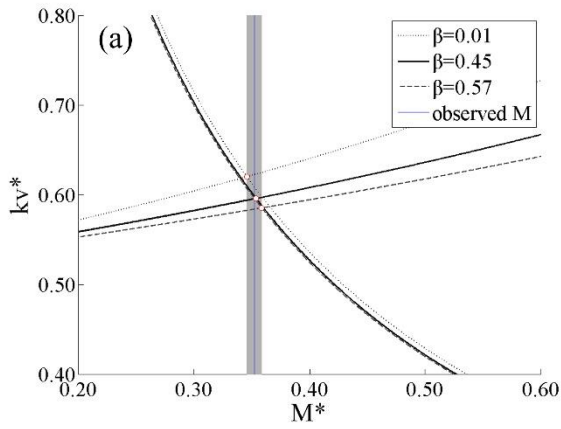
Figure 5: *M** changes with *β*, *LAI* and *h*ₛ*/h* ((a) ~ (c) grassland; (d) ~ (f) forest). The shaded areas mean the range of M* with the change of climate factors.
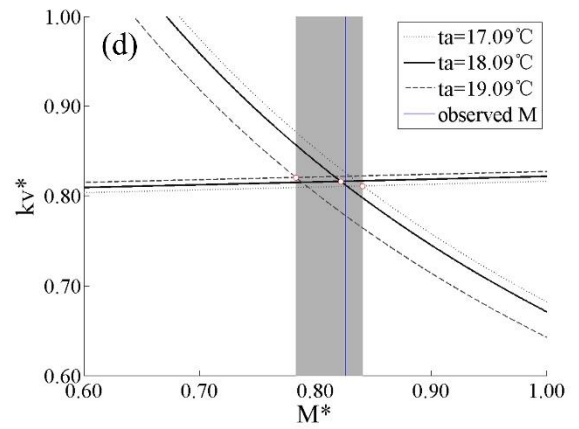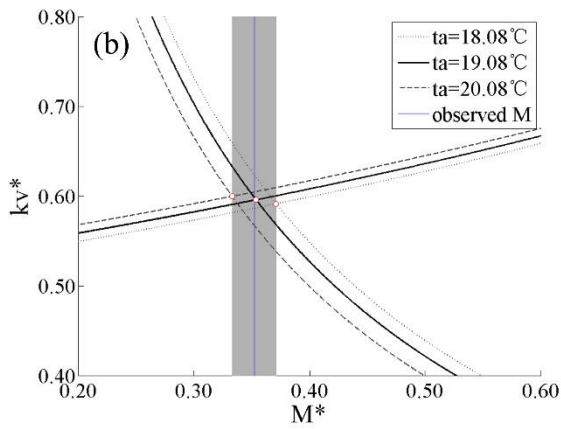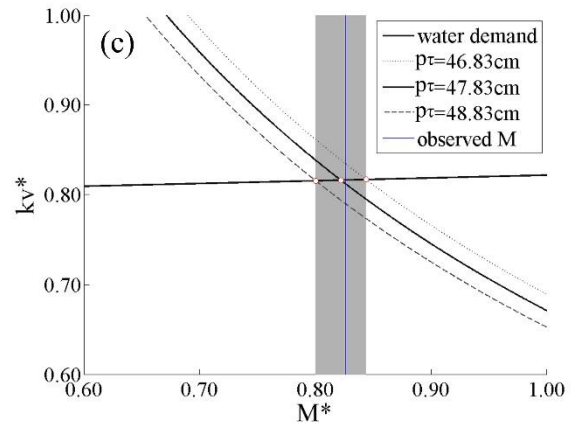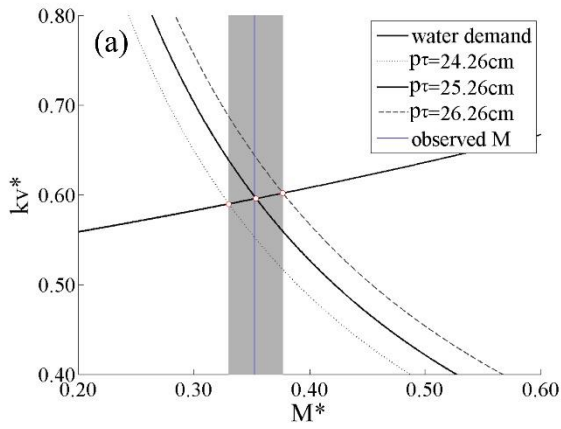
Figure 6: *M** **changes with precipitation (***P_τ***) and air temperature (***t_a***) ((a) ~ (b) grassland; (c) ~ (d) forest). The shaded areas mean the range of M* with the change of vegetation properties.**